ECS Transactions, 35 (2) 17-25 (2011)
10.1149/1.3568844 ©The Electrochemical Society

Green Laser Crystallization of GeSi thin Films and Dopant Activation

Balaji Rangarajan[1], Ihor Brunets[1], Peter Oesterlin[2],
Alexey Y. Kovalgin[1] and Jurriaan Schmitz[1]

[1] MESA+ Institute for Nanotechnology, University of Twente,
P.O. Box 217, 7500AE Enschede, The Netherlands
[2] INNOVAVENT GmbH, Bertha-von-Suttner Str. 5, 37085 Gottingen, Germany

Laser-crystallization of amorphous $Ge_{0.85}Si_{0.15}$ films is studied, using green laser scanning and preformed topography to steer the crystallization. Large crystals (8x2 μm^2) are formed with location-controlled grain boundaries. The obtained films were characterized using Scanning Electron Microscopy, Transmission Electron Microscopy, Atomic Force Microscopy, X-Ray Photoelectron spectroscopy, X-Ray Diffraction and Spectroscopic Ellipsometry. In addition, the activation of ion-implanted poly-$Ge_{0.85}Si_{0.15}$ films is compared after furnace annealing, rapid thermal annealing and green-laser annealing.

Introduction

The CMOS-backend-compatible deposition temperature (400-450 °C) of germanium-silicon (GeSi) alloys has triggered renewed interest in such layers for integrated circuits lately (1). These alloys can be proposed in various 3D integration schemes such as 3D monolithic integration (2, 3). The context of the present work is in infrared detection, where the tunable band gap is an attractive feature of the alloy (4). Doping and crystallinity then become the key issues. Randomly positioned grain boundaries can affect the electrical characteristics of the devices such as thin film transistors fabricated on poly-GeSi films as shown earlier with silicon (5).

In this paper we employ green-laser crystallization to create large grained poly-$Ge_{0.85}Si_{0.15}$ films. Using pre-patterned a-$Ge_{0.85}Si_{0.15}$ lines, the location of grain boundaries can be steered. We further study green-laser annealing for the activation of both p-type and n-type dopants in LPCVD poly-$Ge_{0.85}Si_{0.15}$ films.

Experiment

Thermal oxide of a thickness of 450 nm was grown on top of the Si substrates using wet oxidation. This was followed by the deposition of a-$Ge_{0.85}Si_{0.15}$ and poly-$Ge_{0.85}Si_{0.15}$ films using a custom-built Low Pressure Chemical Vapour Deposition (LPCVD) system with a horizontal furnace used for batch deposition with a base pressure of 10^{-3} mbar. The furnace is heated using resistive heating and the (4-inch) wafers are loaded directly into the furnace on a quartz wafer-boat. SiH_4 and GeH_4 were used as the precursor gases. The

Downloaded 27 Jul 2011 to 130.89.194.102. Redistribution subject to ECS license or copyright; see http://www.ecsdl.org/terms_use.jsp

a-$Ge_{0.85}Si_{0.15}$ films were deposited at 430 °C using 74.8 sccm of SiH_4 flow and 37 sccm of GeH_4 flow with a total pressure of 6 mbar. The poly-$Ge_{0.85}Si_{0.15}$ films were obtained using the same set of parameters except for a total pressure of 0.2 mbar. Prior to each GeSi deposition, a few nanometers of a-Si were deposited using the same LPCVD system in order to form nucleation sites for the subsequent $Ge_{0.85}Si_{0.15}$ deposition. The a-$Ge_{0.85}Si_{0.15}$ films were used for laser crystallization while poly-$Ge_{0.85}Si_{0.15}$ films were used as a reference material as well for doping and activation experiments.

The green laser (515 nm) crystallization involved two different approaches. The first one incorporated direct crystallization of 100nm thick a-$Ge_{0.85}Si_{0.15}$ films using green laser (Fig. 1a). In the second approach, the substrate was covered with 50-nm thick a-$Ge_{0.85}Si_{0.15}$ lines, deposited by LPCVD and patterned using Hydrofluoric Acid-Nitric Acid-Acetic Acid (HNA) solution diluted with De-Ionized (DI) water to form approx. 900 nm wide periodic lines with a pitch of 3 µm. Further 100 nm of a-$Ge_{0.85}Si_{0.15}$ film were deposited on top of these lines, creating the topography as shown in Fig 1b.

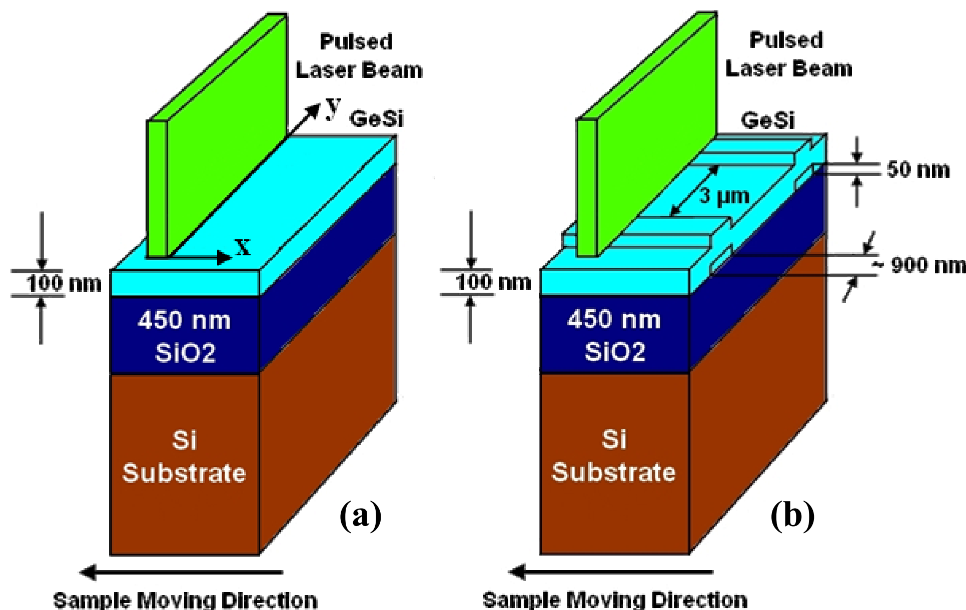

Fig 1: Overview of Laser Crystallization (a) without lines (approach 1) and (b) with pre-patterned lines (approach 2).

The pre-patterned a-$Ge_{0.85}Si_{0.15}$ lines lead to a lateral, periodic temperature gradient, causing crystallization to start in predefined locations. As a result, the location of the dominant grain boundaries should be dictated by the location of the preformed lines.

The green laser beam was pulsed at a frequency of 10 kHz with the pulse duration of 285 ns. The x-axis of the laser beam showed a Gaussian profile with Full Width Half Maximum (FWHM) set at 15 µm whereas the y-axis showed a uniform profile with FWHM set at approx. 2 mm (see Fig 1).

Downloaded 27 Jul 2011 to 130.89.194.102. Redistribution subject to ECS license or copyright; see http://www.ecsdl.org/terms_use.jsp

The samples were moved unidirectional under the pulsed laser beam. The scanning speed was adjusted to achieve the required overlapping of consecutive laser pulses. This overlapping was required for lateral growth during the crystallization process. Overlappings of 98% and 95% were chosen on the basis of a set of initial trials for all the following crystallization experiments. The same settings were used on samples with, and without preformed lines. The samples were moved particularly along the direction of the pre-patterned lines (as shown in Fig. 1b).

The laser energy density was optimized for each of the two overlapping settings using a set of experiments wherein the laser energy densities were increased in small steps from 0.4 Jcm^{-2} until layer evaporation was observed. Laser energy densities of 1.2 and 1.3 Jcm^{-2} were found to provide the best results of crystallization.

All the films were characterized using Scanning Electron Microscopy (SEM), Transmission Electron Microscopy (TEM), Atomic Force Microscopy (AFM), X-Ray Photoelectron Spectroscopy (XPS), X-Ray Diffraction (XRD) and Spectroscopic Ellipsometry (SE).

To study $Ge_{0.85}Si_{0.15}$ doping, BF_2^+, As^+ and P^+ were ion-implanted into 100 nm of LPCVD poly-$Ge_{0.85}Si_{0.15}$ films with a variety of implantation conditions. Boron was implanted at 30 and 55 keV to a dose of $1x10^{15}$ cm^{-2}. Arsenic was implanted at 40 and 55 keV, and phosphorous at 40 and 50 keV. Three implantation doses were used for As and P: $4x10^{14}$ cm^{-2}, $1x10^{15}$ cm^{-2} and $4x10^{15}$ cm^{-2}. The implantation was followed by dopant activation using either furnace annealing, rapid thermal annealing (RTA) or green-laser annealing.

Results and Discussions

Green laser crystallization

There is a growing interest in making good quality Ge and GeSi alloy films. Significant work has already been done in this field using an (UV) excimer laser (6, 7).

The SEM image (Fig. 2a) of the laser crystallized film clearly shows the formation of large, elongated grains typically 8 µm in length and 2 µm in width. This has been observed for both overlappings of 95% and 98%. A comparison between Fig. 2a and Fig. 2b clearly shows that the pre-patterned a-$Ge_{0.85}Si_{0.15}$ lines (indicated by dotted lines in Fig. 2a) influence the size, shape and direction of the crystal grains.

On the other hand, direct crystallization of a-$Ge_{0.85}Si_{0.15}$ films resulted in the random formation of grains as seen from SEM image in Fig 2b. This highlights the advantage of using pre-patterned lines during the crystallization process. The grains are more randomly directed; the size of a typical grain was still in the range of 8 µm in length and up to 1 µm in width.

Downloaded 27 Jul 2011 to 130.89.194.102. Redistribution subject to ECS license or copyright; see http://www.ecsdl.org/terms_use.jsp

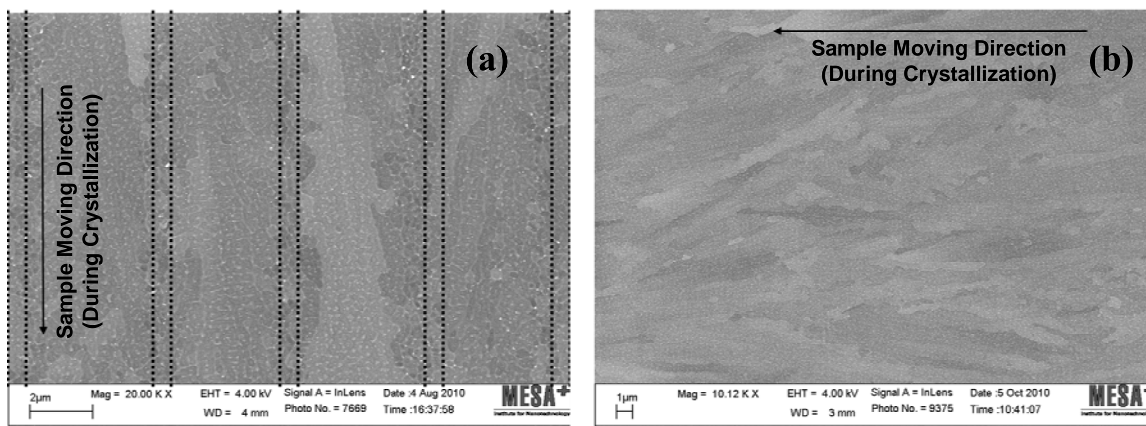

Fig. 2: (a) SEM top view of laser crystallized film with pre-patterned lines; pre-patterning is indicated by the vertical dotted lines. (b) same, without pre-patterned lines.

The trend observed in the formation of grains in laser crystallized $Ge_{0.85}Si_{0.15}$ with pre-patterned lines was opposite to that observed in the earlier work on laser crystallization of a-Si (8). Namely, in (8) it was observed that the grain centers are positioned on the lines and the grain boundaries are mostly located between the lines. It can be seen from the SEM image (Fig. 2a) that, in case of $Ge_{0.85}Si_{0.15}$, the grains originate anywhere in between the lines and extend further until they are terminated at the pre-patterned lines. This opposite behavior can be attributed to a difference in the thermal and optical properties between a-$Ge_{0.85}Si_{0.15}$ and a-Si. Additional study is required to further clarify this effect.

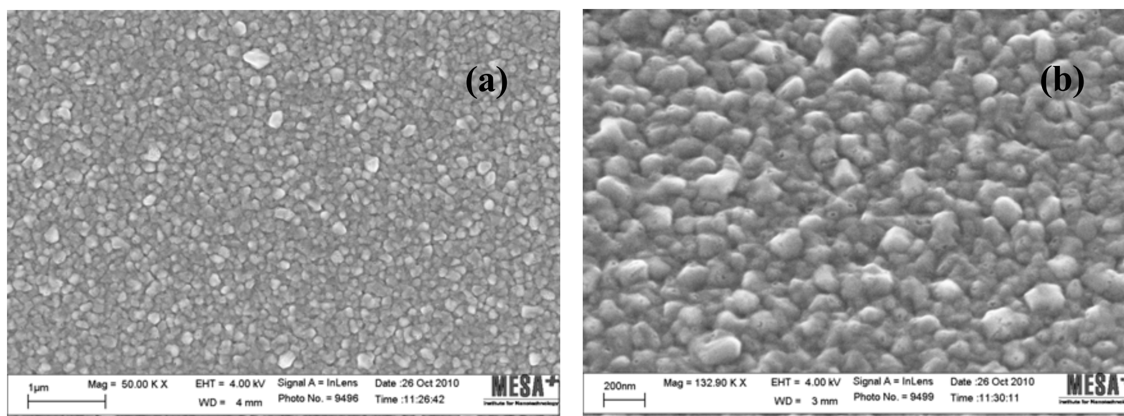

Fig. 3: SEM images of the reference LPCVD poly-$Ge_{0.85}Si_{0.15}$ films: (a) top view; (b) tilted view at 50°.

When compared to the laser crystallized films, the reference (i.e., as-deposited) LPCVD poly-$Ge_{0.85}Si_{0.15}$ films show smaller grains with a typical size of 200 nm (Fig. 3). From the results of AFM, the RMS value of roughness for the reference poly-$Ge_{0.85}Si_{0.15}$ was found to be approximately 12.6 nm compared to that of 2.5 nm for a laser crystallized $Ge_{0.85}Si_{0.15}$ film.

Downloaded 27 Jul 2011 to 130.89.194.102. Redistribution subject to ECS license or copyright; see http://www.ecsdl.org/terms_use.jsp

The TEM and SEM cross-section images (Fig. 4) depict that the laser crystallized films do not contain any amorphous residual along its depth after the crystallization process i.e. the entire film has been crystallized from top to bottom. As also seen from TEM images (Fig. 4), there are no structural deformities such as voids (generally depicted as bright spots) at the interface between GeSi and thermal SiO_2. There are also a few nanometers of a mixture of germanium and silicon oxides (as shown by XPS in Fig. 6), formed on the top of the laser crystallized film during the crystallization process, as the crystallization was done in an open chamber exposed to atmospheric air.

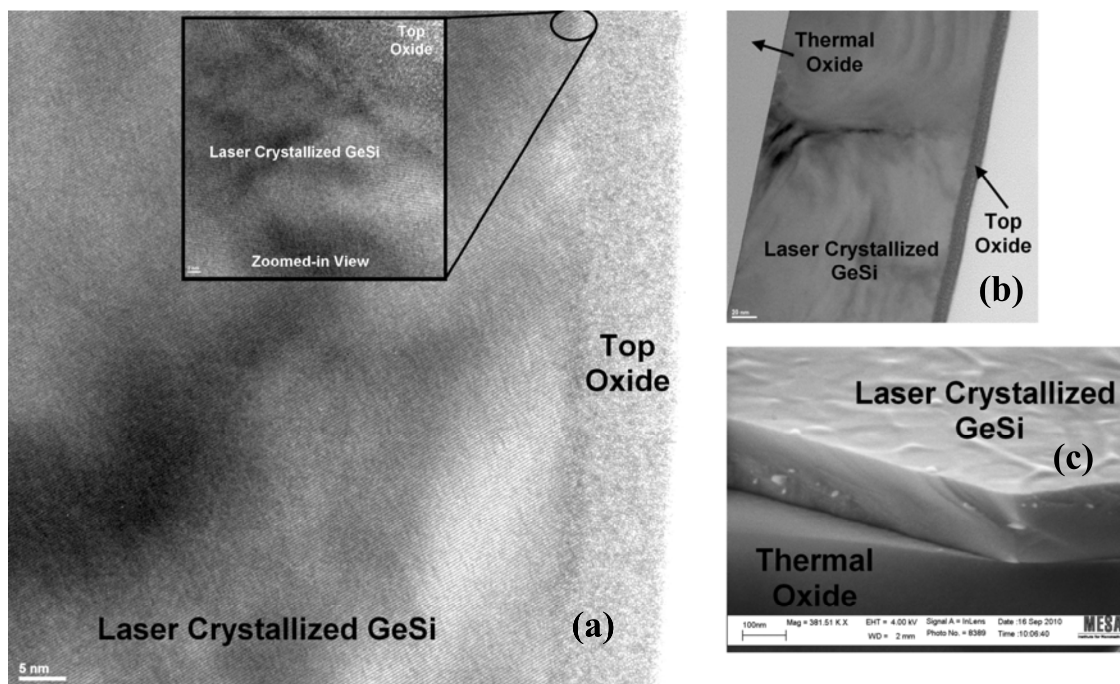

Fig. 4: (a) A TEM cross-section of laser crystallized $Ge_{0.85}Si_{0.15}$; (b) A TEM overview at the $GeSi/SiO_2$ interface (c) SEM cross-section of laser crystallized GeSi.

In order to determine the crystallinity of the material and the effect of the laser treatment, XRD was performed on both the reference (i.e., LPCVD-poly) and laser crystallized $Ge_{0.85}Si_{0.15}$ films (Fig. 5). Note the prominence of (311) 2θ peaks of laser crystallized $Ge_{0.85}Si_{0.15}$ films, a thousand times higher than that for LPCVD poly-$Ge_{0.85}Si_{0.15}$ film, while Fig. 5b shows that the (311) 2θ peak of the laser crystallized $Ge_{0.85}Si_{0.15}$ film with pre-patterned lines is twice as much as the one without the lines. Second, the other 2θ peaks for (111) and (220) for laser crystallized $Ge_{0.85}Si_{0.15}$ films are much smaller when compared to that for LPCVD poly-$Ge_{0.85}Si_{0.15}$ film, clearly indicating the dominance of (311) 2θ peak for laser crystallized $Ge_{0.85}Si_{0.15}$ films. Finally, a clear shift of the (311) 2θ peak position for the laser crystallized $Ge_{0.85}Si_{0.15}$ films can also be observed. Generally, such a peak for poly-Ge_xSi_{1-x} should lie between 56.13° and 53.68°, which represents the (311) 2θ peak positions for Si and Ge, respectively. For Ge-rich alloys, the peak position should be nearer to that of pure germanium. In case of our laser crystallized $Ge_{0.85}Si_{0.15}$, it stands at 56.47°, which has far-exceeded the peak position value for Si. This indicates internal compressive stress in the layer.

Downloaded 27 Jul 2011 to 130.89.194.102. Redistribution subject to ECS license or copyright; see http://www.ecsdl.org/terms_use.jsp

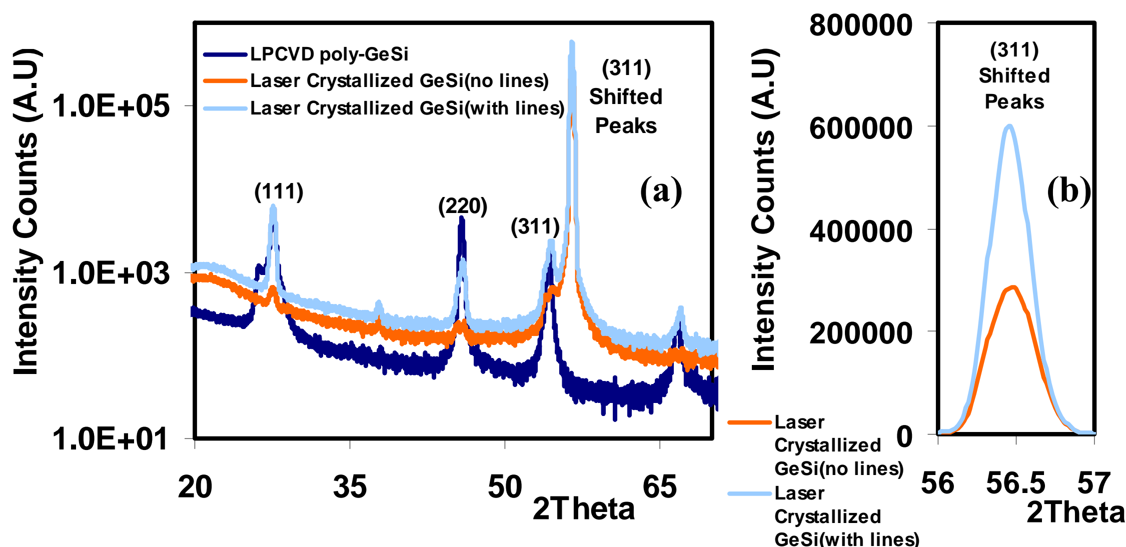

Fig. 5: (a) XRD graph for LPCVD-poly and laser-crystallized $Ge_{0.85}Si_{0.15}$ films (b) (311) 2θ peaks of the laser crystallized $Ge_{0.85}Si_{0.15}$ films with and without pre-patterned lines.

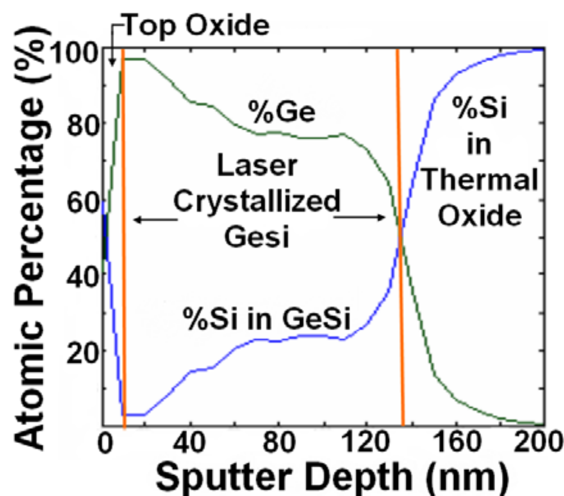

Fig. 6: XPS Depth profile for laser crystallized $Ge_{0.85}Si_{0.15}$.

The internal stress can be attributed to non-uniformity in the composition of $Ge_{0.85}Si_{0.15}$ along the depth of the film as seen from the XPS (Fig. 6). The XPS results of laser crystallized $Ge_{0.85}Si_{0.15}$ films (with and without pre-patterned lines) show good uniformity in composition laterally across the film (i.e., wafer surface) but not vertically. The top layer was enriched with Ge compared to the bottom (Fig. 6). On the other hand, the reference LPCVD poly-$Ge_{0.85}Si_{0.15}$ and the prior-to-crystallization a-$Ge_{0.85}Si_{0.15}$ show good uniformity in the composition along the depth of the film (as well as laterally across the film). This indicates that the observed non-uniformity is a result of the laser crystallization and not the deposition.

Downloaded 27 Jul 2011 to 130.89.194.102. Redistribution subject to ECS license or copyright; see http://www.ecsdl.org/terms_use.jsp

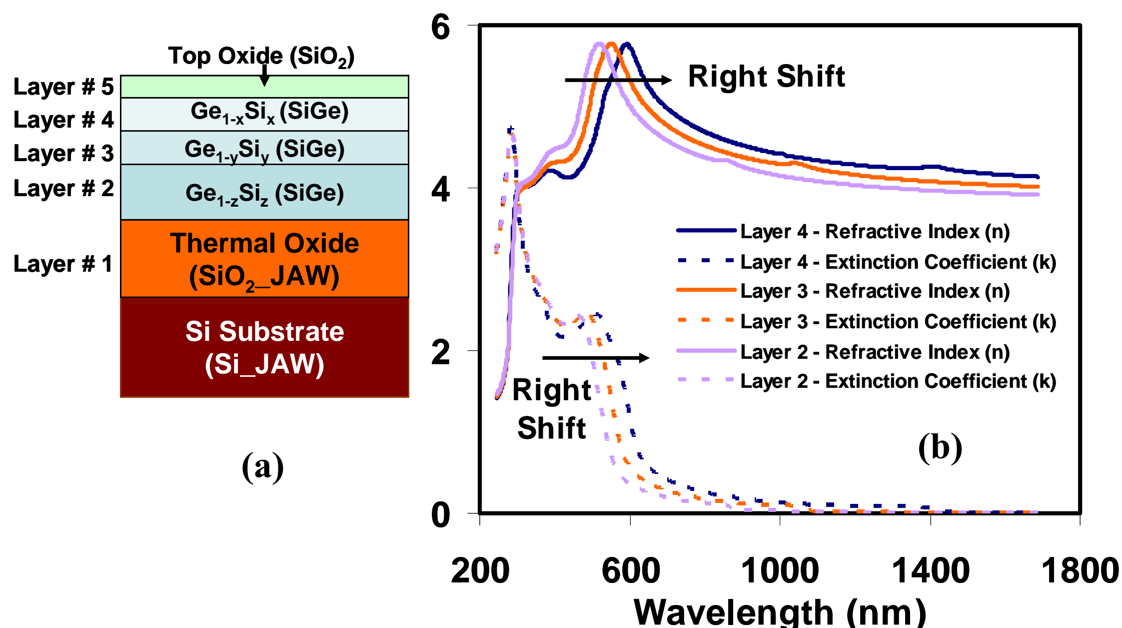

Fig. 7: (a) Model used for fitting data obtained from Spectroscopic ellipsometry (b) The extracted optical constants for layer #2, #3 and #4 with respect to different wavelengths.

The XPS data in Fig. 6 can additionally be verified using the spectroscopic ellipsometry (SE). The model used for fitting data during analysis is shown in Fig. 7a, where the laser crystallized GeSi layer is represented as a three-layer-stack - a simple layout depicting the compositional variance. In Fig. 7b the spectral dependence of the refractive index and extinction coefficient of layers #2, #3 and #4 is shown. As we move from layer #2 to #4, it can be seen that both refractive indices and extinction coefficients show a right shift towards higher wavelengths. This signifies that the germanium fraction increases gradually from layer #2 to #4. Each sub-layer shows different optical constants as a result of the compositional variability in each layer (5). It should also be noted that for the layer #5 we have only used silicon dioxide for fitting purposes. In general, the superficial layer is a mixture of germanium and silicon oxides as seen from XPS (Fig. 6).

Table.1 presents the calculated lattice constant for the laser crystallized $Ge_{0.85}Si_{0.15}$ films and the reference LPCVD poly-$Ge_{0.85}Si_{0.15}$ films. This rough evaluation is based on the XRD data of Fig. 5 and done for a simple analysis purpose as it has to be clearly noted that the reference and laser crystallized films are not similar (see e.g. Fig. 5). We used LPCVD poly-$Ge_{0.85}Si_{0.15}$ as the reference by lack of GeSi material with a prominent (311) face. The lattice constant is 0.21 Å (3.7%) lower in the laser-crystallized film compared to the LPCVD film. This would imply a very high difference in strain. Based on the position of the 2θ peak, it appears that the LPCVD layer has low strain, and the laser-crystallized one has high strain. The vertical non-uniformity in the laser-crystallized layer (Fig. 6) may well be the cause of such high strain, but this requires further study.

Downloaded 27 Jul 2011 to 130.89.194.102. Redistribution subject to ECS license or copyright; see http://www.ecsdl.org/terms_use.jsp

Material Type	(311) 2θ peak	d (Å)	a (Å)	Δa/a (%)
LPCVD Poly $Ge_{0.85}Si_{0.15}$	**54.24°**	**1.69**	**5.59**	**3.7**
Laser crystallized $Ge_{0.85}Si_{0.15}$	**56.47°**	**1.62**	**5.38**	

Table 1: Lattice properties for laser crystallized $Ge_{0.85}Si_{0.15}$ film with respect to LPCVD poly-$Ge_{0.85}Si_{0.15}$ film, based on XRD measurements. *d* is the distance between the lattice planes; *a* is the lattice constant.

Ion Implantation and Dopant Activation

The sheet resistivity was measured using four-point probe method. Low sheet resistivity values (ρ_{sh}) were obtained for boron-implanted layers by using furnace annealing (ρ_{sh} = 0.67x10^{-2} Ω-cm), rapid thermal annealing (ρ_{sh} = 0.55x10^{-2} Ω-cm) and green-laser annealing (ρ_{sh} = 1.1 x10^{-2} Ω-cm); it was instead challenging to obtain low sheet resistivity values for both arsenic and phosphorous implanted layers using furnace and rapid thermal annealing irrespective of the implantation conditions. In case of pure Ge this can be attributed to out-diffusion of n-type dopants and forming shallow n+ junction in Ge can be impaired due to high diffusivities of n-type dopants (As and P) in Ge (9, 10). As LPCVD poly-$Ge_{0.85}Si_{0.15}$ has significant high Ge content, its behavior can therefore be related to that of pure germanium. On the other hand, boron has lower diffusivity in Ge when compared to n-type dopants and the fact that the boron can get activated already during the implantation could explain its easier activation (9). The sheet resistance does not provide information on a possible vertical gradient in the resistivity. Detailed analysis such as secondary ion mass spectroscopy and spreading resistance profiling is required to gain more in-depth view on such issues.

Yet green laser annealing was able to successfully activate both p-type and n-type dopants. For boron the calculated sheet resistivity was ρ_{sh} = 1.1 x10^{-2} Ω-cm while that for arsenic and phosphorous, it was ρ_{sh} = 0.69 x10^{-2} Ω-cm and 3.1 x10^{-2} Ω-cm respectively. The laser annealing uses laser pulses with pulse duration of 285 ns and the frequency was set at 10 kHz. The overlapping was fixed at 95% with a FWHM of 40 μm along the x-axis of the laser beam. The laser energy was fixed at 0.4 Jcm^{-2}. The sub-microsecond pulse duration might prevent the out-diffusion mentioned above. This still needs further investigation.

Conclusions

Green laser crystallization of a-$Ge_{0.85}Si_{0.15}$ films combined with pre-patterned a-$Ge_{0.85}Si_{0.15}$ lines during the crystallization process showed the formation of large grains typically 8 μm long and 2 μm wide contained between the pre-patterned lines thereby making it easier to locate such grains during further fabrication processes. Direct crystallization of a-$Ge_{0.85}Si_{0.15}$ film without pre-patterned lines resulted in the formation of randomly positioned grains. Controlling the grain boundary position with

Downloaded 27 Jul 2011 to 130.89.194.102. Redistribution subject to ECS license or copyright; see http://www.ecsdl.org/terms_use.jsp

pre-patterned lines likely enhances the characteristics of devices positioned properly on such films.

Green laser (515 nm) anneals properly activate both p-type (boron) and n-type (arsenic and phosphorous) dopants in LPCVD poly-$Ge_{0.85}Si_{0.15}$ films whereas both furnace annealing and RTA have failed in successfully activating the n-type dopants.

For low-temperature fabrication of electronic devices, such as CMOS post-processing or 3D integration requiring good quality semiconductor materials, green laser crystallization of $Ge_{0.85}Si_{0.15}$ seems a good candidate.

Acknowledgements

The authors gratefully acknowledge the support of the Smart Mix Programme of the Netherlands Ministry of Economic Affairs and the Netherlands Ministry of Education, Culture and Science. The authors would like to thank Tom Aarnink (LPCVD), Jiwu Lu & Giulia Piccolo (XRD), Lan Anh Tran (AFM), Gerard Kip (XPS), Rico Keim (TEM) and Mark Smithers (SEM), all from MESA+ Institute for Nanotechnology, University of Twente, for their support.

References

1. Fedder G.K *et al.*, “Technologies for Cofabricating MEMS and Electronics” *in Proc. Of IEEE, Vol.96, No. 2, Feb. 2008, pp. 306-322.*
2. Yuan Xie, “Processor Architecture Design Using 3D Integration Technology”, *23rd International Conference on VLSI Design, DOI 10.1109/VLSI.Design.2010.60.*
3. M. Vinet *et al.*, “3D monolithic integration: Technological challenges and electrical results”, *Microelectronic Engineering (2010), DOI:10.1016/j.mee.2010.10.022.*
4. “Properties of Strained and Relaxed Silicon Germanium”, edited by Erich Kasper, *pp. 123-129, 1995: INSPEC, ISBN 0 85296 826 4.*
5. R. Ishihara, "Effects of grain-boundaries on excimer-laser crystallized poly-Si thin-film transistors*", Proc. AMLCD Tech. Dig., pp. 259 2001.*
6. Tao Chen *et al.*, “High Performance Single-Grain Ge TFTs without Seed Substrate”, *IEDM 2010, pp. 496-499, IEEE International.*
7. Ishihara. R *et al.*, M, “Excimer-Laser Crystallization of Silicon-Germanium”, *Solid State Device Research Conference, pp. 1075 – 107, 1996. ESSDERC '96.*
8. I. Brunets *et al.*, “Low temperature Fabricated TFTs on Polysilicon Stripes” *Vol. 56, pp. 1637-1644 Aug 2009 in IEEE Transactions on Electron Devices.*
9. E. Simoen *et al.*, “Ion-implantation issues in the formation of shallow junctions in germanium” *Materials Science in Semiconductor Processing 9 (2006) 634–639.*
10. A. Axmann *et al.*, “Implantation Doping of Germanium with Sb, As, and P”, *Applied Physics 12, pp. 173-178 (1977).*

Downloaded 27 Jul 2011 to 130.89.194.102. Redistribution subject to ECS license or copyright; see http://www.ecsdl.org/terms_use.jsp